Electronic Supplementary Material (ESI) for Nanoscale.
This journal is © The Royal Society of Chemistry 2020

Supporting Information for

X-ray recharged long afterglow luminescent nanoparticles $MgGeO_3$: Mn^{2+}, Yb^{3+}, Li^+ in the first and second biological windows for long-term bioimaging

Shenghui Zheng,[a, b] Junpeng Shi,[a] Xiaoyan Fu,[c,*] Chengcheng Wang,[a, b] Xia Sun,[a] Changjian Chen,[d] Yixi Zhuang,[d] Xianyan Zou,[a] Yuechan Li,[c] Hongwu Zhang[a, *]

a) Key Lab of Urban Pollutant Conversion, Institute of Urban Environment, Chinese Academy of Sciences, Xiamen, 361021, China

b) University of Chinese Academy of Sciences, No. 19A Yuquan Road, Beijing, 100049, China

c) College of Materials Science and Engineering, Key Laboratory of Functional Materials and Applications of Fujian Province, Xiamen University of Technology, Xiamen 361024, China

d) College of Materials, Xiamen University, Simingnan Road 422, Xiamen 361005, P. R. China

Corresponding author:

E-mail: fuxiaoyan@xmut.edu.cn;

E-mail: hwzhang@iue.ac.cn.

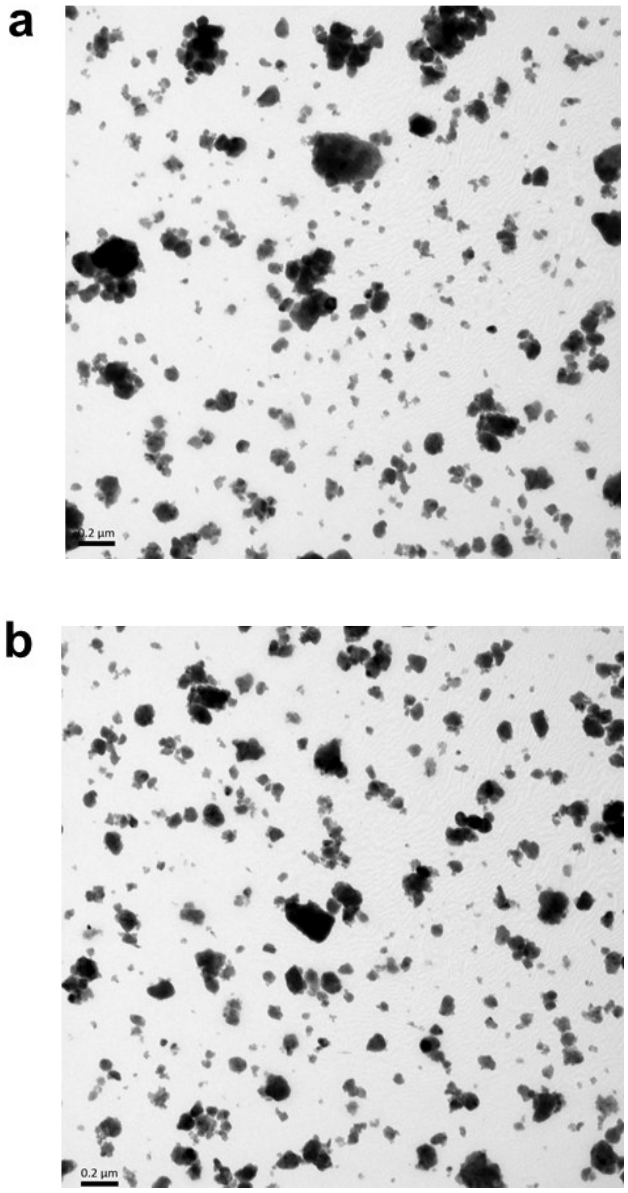

Figure S1. (a)-(b) TEM images of as-prepared MGO nanoparticles without further centrifugal screening.

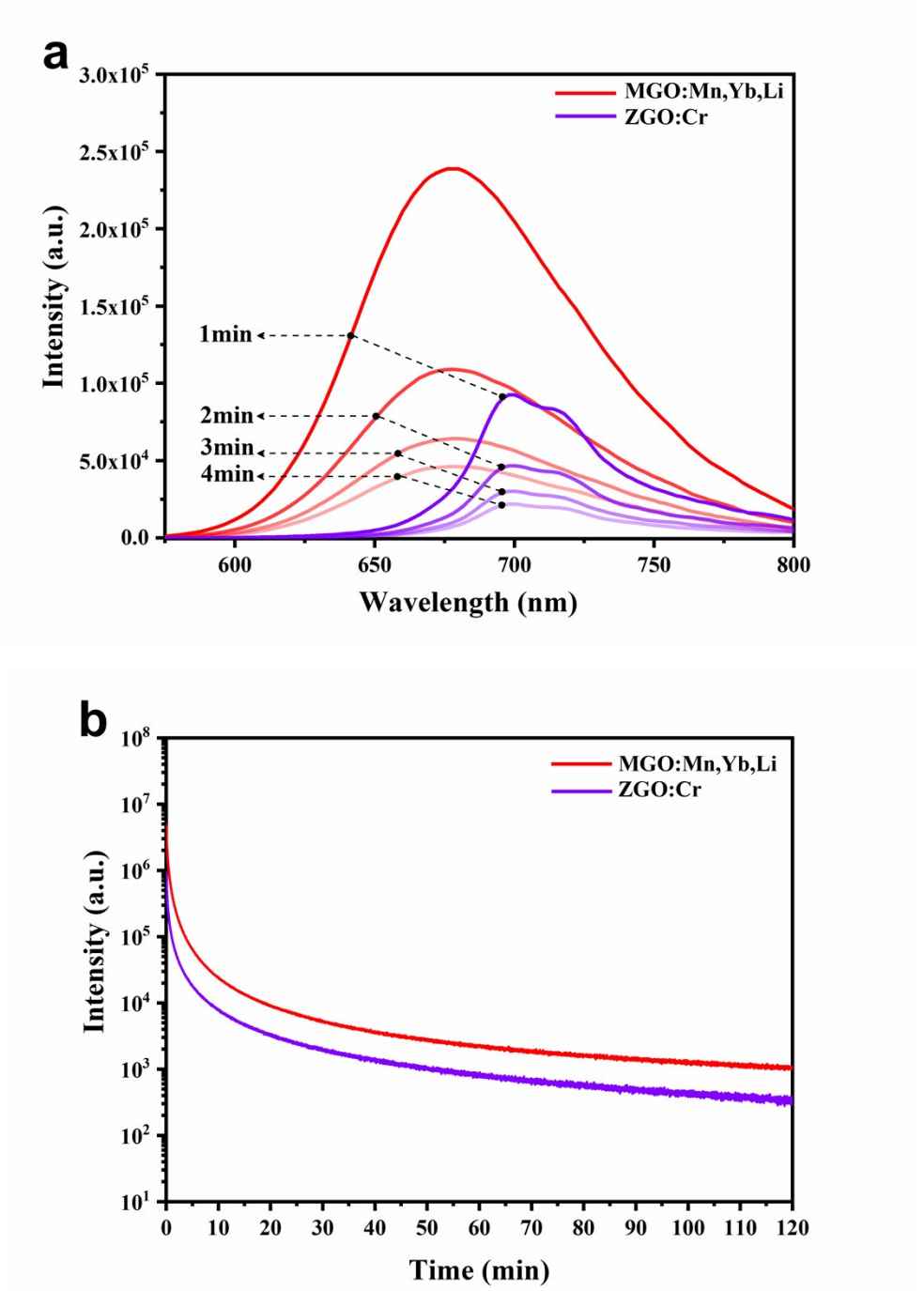

Figure S2. (a) Persistent luminescence spectra of $MgGeO_3$:Mn^{2+}, Yb^{3+}, Li^+ (red lines) and $ZnGa_2O_4$: Cr^{3+} (purple lines) at 10 s after 2 min of UV irradiation. (b) Persistent luminescence decay curve of $MgGeO_3$: Mn^{2+}, Yb^{3+}, Li^+ (red lines) and $ZnGa_2O_4$: Cr^{3+} (purple lines) after 5 min of UV irradiation.

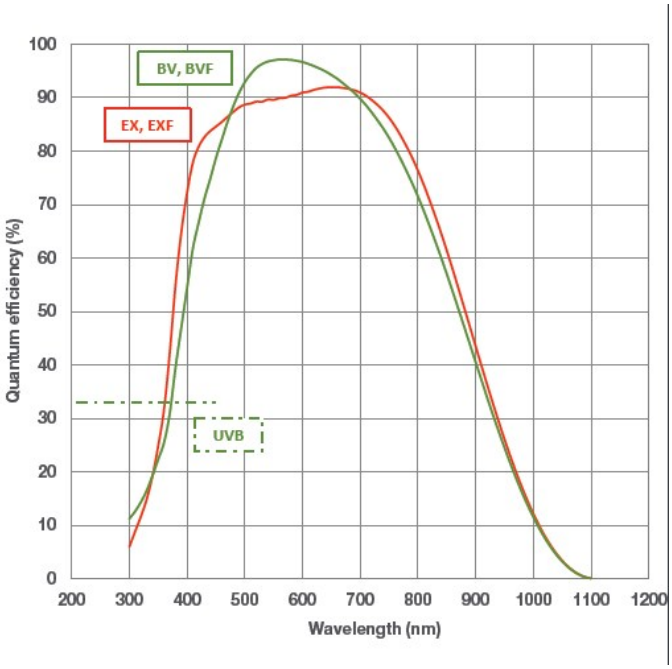

Figure S3. The quantum efficiency of CCD camera.

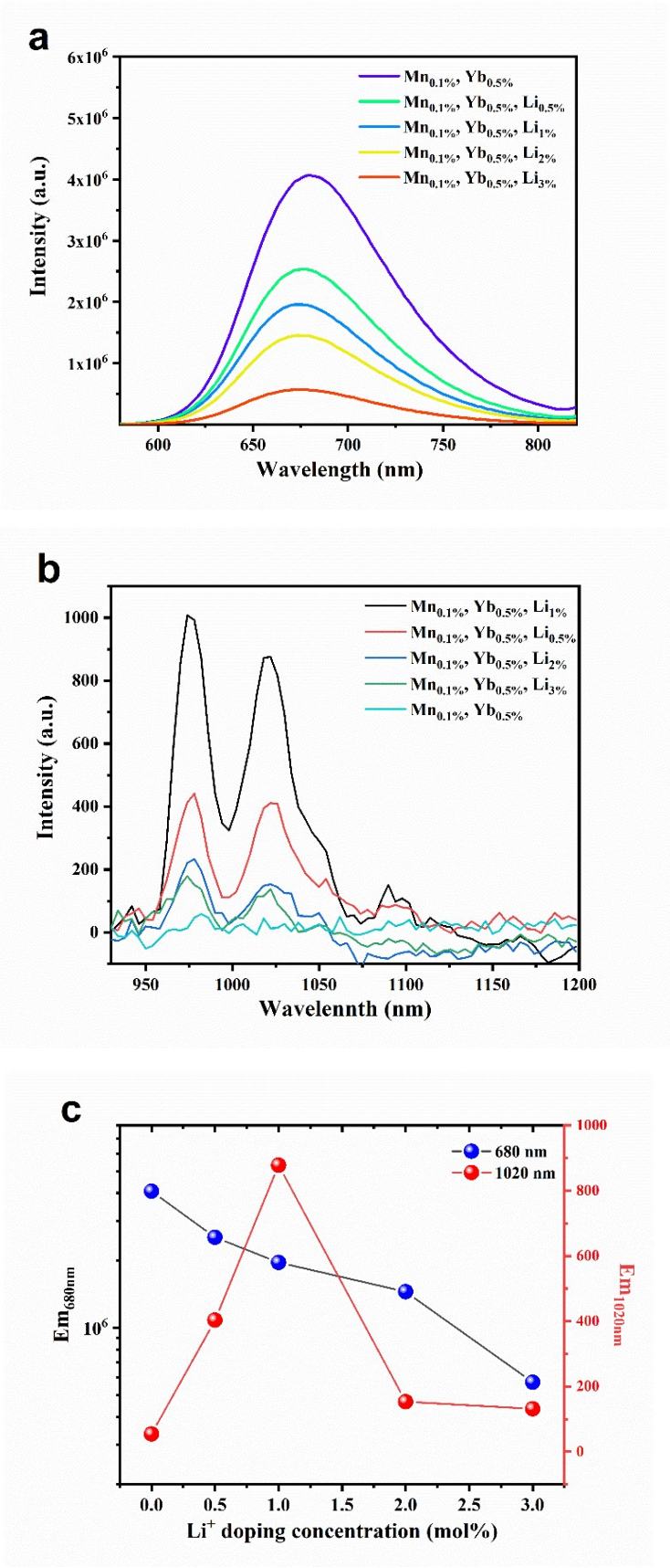

Figure S4. (a) NIR-I persistent luminescence spectra of $MgGeO_3$:$Mn_{0.1\%}$, $Yb^{3+}_{0.5\%}$, Li^{+}_{x} (x=0- 3 mol %) monitored at 680 nm after 254 nm UV irradiation for 2 min. (b) NIR-II persistent luminescence emission

spectra recorded at 5 s after 2 min irradiation of 254 nm. (c) The relationship between persistent luminescence intensity of MGO and the concentration of Li^+.

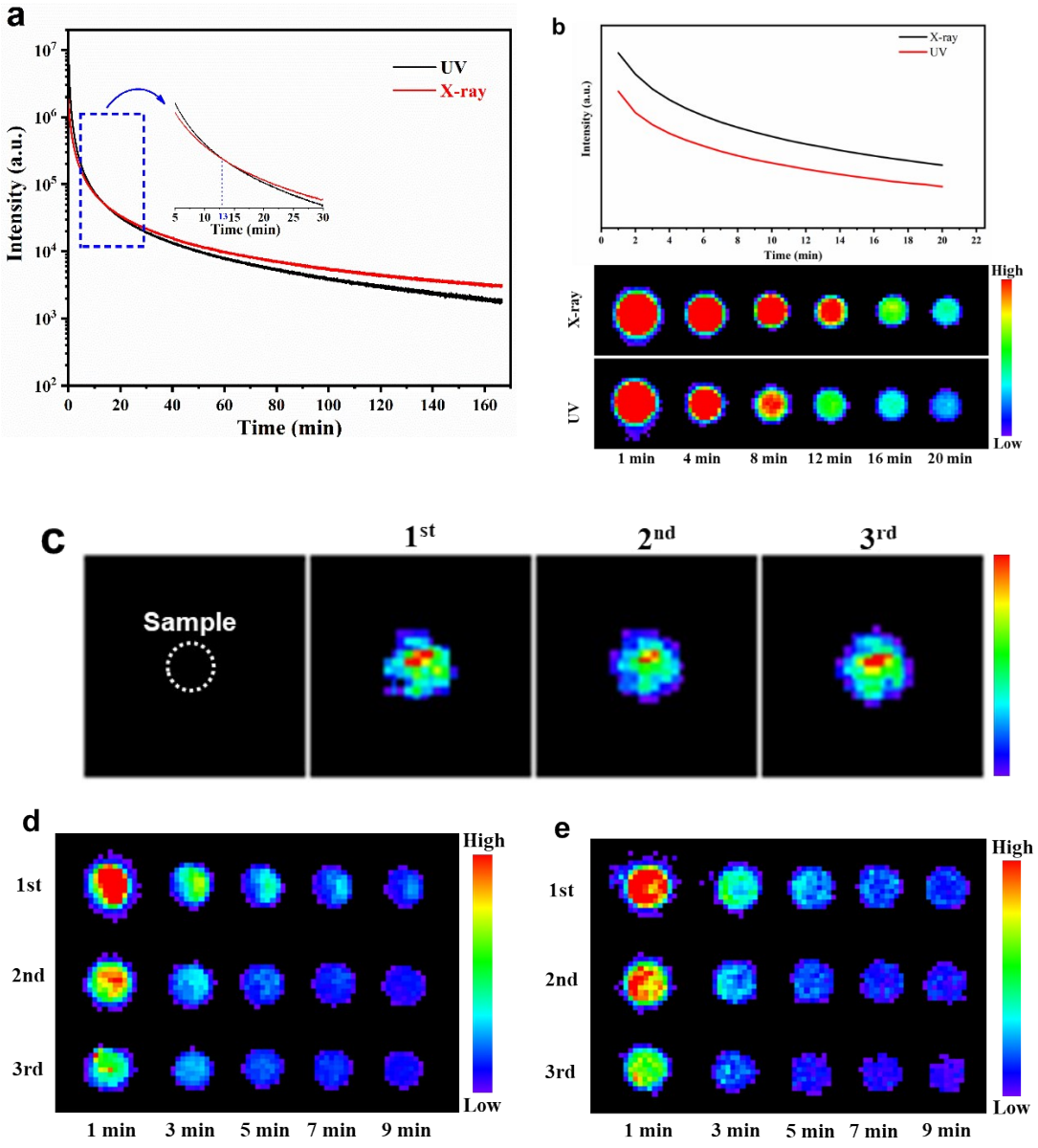

Figure S5. (a) Comparison of persistent luminescence intensity under X-ray ($62.9\ mW/cm^2$) and UV ($80mW/cm^2$) irradiation for 2 min, respectively. (b) persistent luminescence signal beyond 980 nm after recharging by X-ray and UV. (c) persistent luminescence signal of MGO beyond 980 nm for three charged cycles with X-ray. (d)-(e) persistent luminescence signal of MGO beyond 980 nm after stopping initial X-ray irradiation for 2 h and then were *in situ* photo-stimulated by 650 nm and 808 nm laser for three imaging cycles.

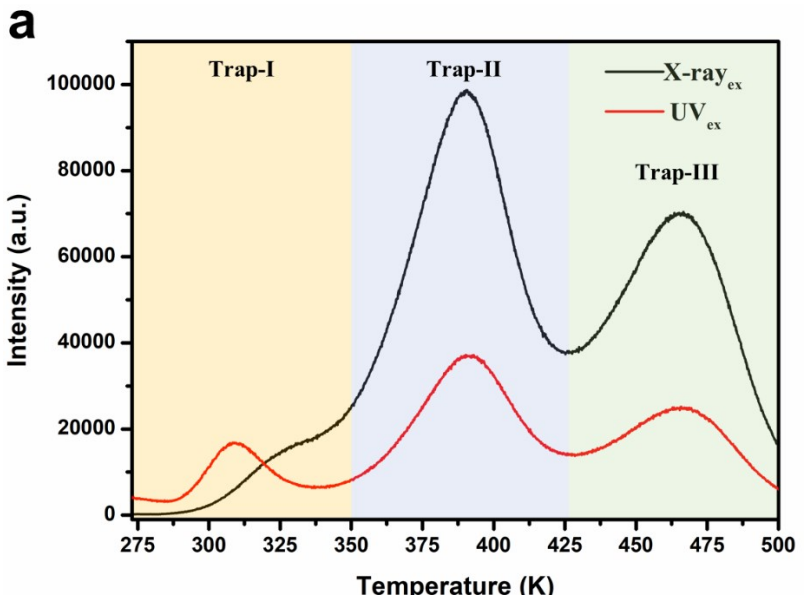
a
Trap-I
Trap-II
Trap-III
X-ray$_{ex}$
UV$_{ex}$
Intensity (a.u.)
Temperature (K)

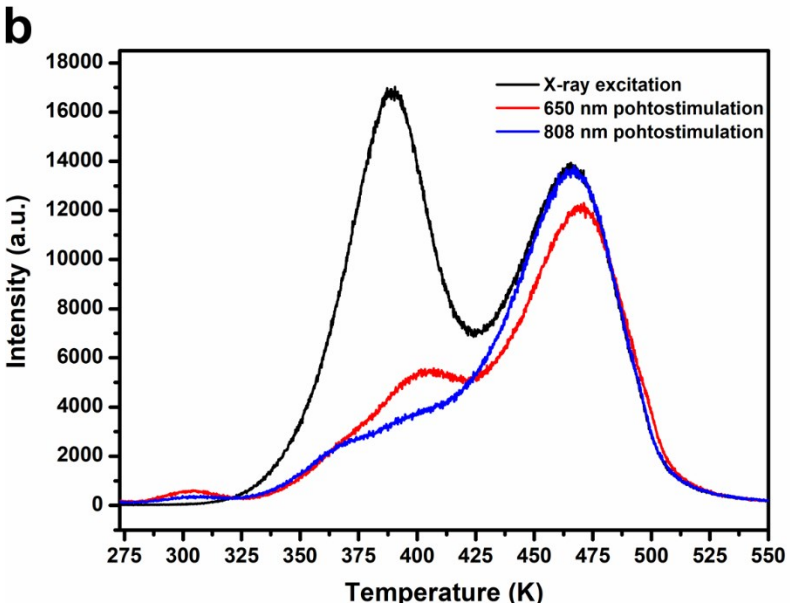
b
X-ray excitation
650 nm pohtostimulation
808 nm pohtostimulation
Intensity (a.u.)
Temperature (K)

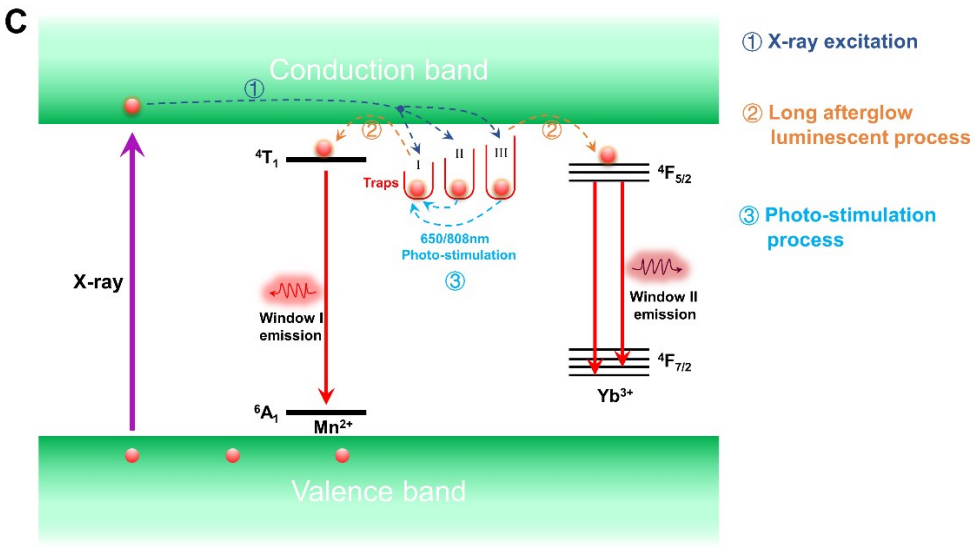

Figure S6. (a) Thermoluminescence curves of MGO powder under X-ray ($62.9\ mW/cm^2$; black line) and UV excitation ($80mW/cm^2$; red line), respectively. (b) The MGO sample under X-ray charging 2min with 130 min waiting (black line) and photo-stimulation by 650 nm laser for 3 min at 273 k after X-ray excitation with 120 min waiting (red line), photo-stimulation in the same condition with 808 nm laser (blue line). (c) The schematic diagram of long persistent luminescence process in the MGO matrix.

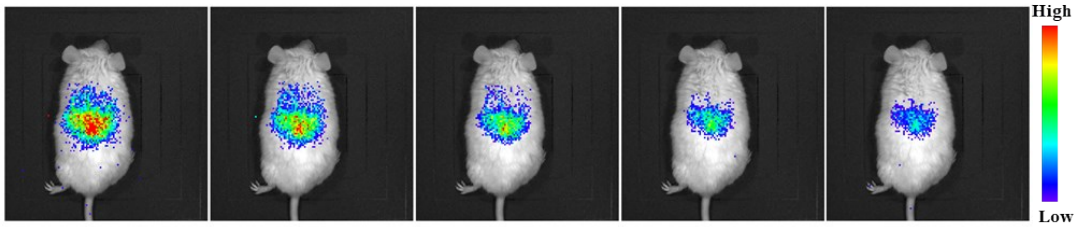

Figure S7. *in vivo* imaging excited by X-ray after intravenously injected in a normal mouse.